OUT-OF-PLANE SEISMIC EVALUATION AND RETROFIT OF TURN-OF-THE-CENTURY NORTH AMERICAN MASONRY WALLS

By Jocelyn Paquette,[1] Michel Bruneau,[2] Member, ASCE, and André Filiatrault,[3] Member, ASCE

ABSTRACT: Three masonry walls with their wood backing were extracted from an old three-story residential building. These specimens are representative of a type of construction widely used in North America circa 1900, in which a single wythe exterior masonry wall was tied only with nails to the timber structure, leaving an irregular gap between the masonry and timber walls. To seismically retrofit such buildings, special seismic-resistant anchorage of the walls would be required at every floor at a minimum. Questions remained, however, as to the out-of-plane resistance of the remaining walls spanning between floors. To partly answer these questions, the three specimens extracted from the existing building were tested using a shake table, submitting them to multiple ground motions of progressively larger intensity until structural failure. These tests have demonstrated that such walls could resist significant out-of-plane inertial accelerations without failure. Performance can be increased by different retrofit methods such as providing anchors at midheight to force the wood and masonry wall to move as a unit, and adding fiberglass strips epoxied to the masonry wall to increase its out-of-plane stiffness and strength.

INTRODUCTION

A construction technique widely used for the facade and common walls of many older (circa 1900) residential buildings in North America consisted of laying a single wythe exterior masonry wall along the wood structure. This was partly done as a fire-propagation prevention measure in dense urban areas. Generally, the wood building would consist of stacked rough-cut timber planks laterally supported by vertical (wind) posts. The masonry walls typically resisted their own weights over the height of the building (typically three to four stories) and were tied only with nails to the wood backing. The nail heads were embedded in mortar joints, every four or five brick layers, and spaced horizontally at approximately 300 mm. This construction procedure left an irregular gap between the masonry and the timber wall.

Such buildings have been constructed in parts of eastern North America where large but infrequent earthquakes are expected to occur. It has been repeatedly shown, following earthquakes worldwide, that unreinforced masonry walls can be particularly vulnerable to strong ground shaking, and the type of construction described above should be no exception. It may thus be assumed that, as a minimum seismic retrofit measure, walls would have to be anchored at the floor/roof levels using standard seismic-resistant details [e.g., as specified in International (1997)]. However, because the interaction between the masonry and timber backing is not well understood for this type of construction subjected to out-of-plane seismic excitation, questions arise as to whether it is also necessary to retrofit the walls between floors. In particular, having access to only one side of the masonry surface may require that new retrofit schemes be developed. Given that such buildings commonly provide low-cost housing in regions of low seismic awareness, excessive structural interventions are unlikely to be implemented.

With that perspective, out-of-plane shake table tests were conducted on three unreinforced masonry walls and wood backing assemblies extracted from an older existing residential building. The availability of this building provided a special opportunity, since reproducing the actual conditions and properties of these older structures with new materials in the laboratory would have been difficult. The first wall was tested in its existing condition, while the two others were retrofitted with different methods prior to testing. This paper discusses these experimental findings, and investigates the adequacy of various analytical procedures to explain the observed behavior.

SPECIMEN RETRIEVAL AND PROPERTIES

The three wall specimens were extracted from an old three-story building in Montreal, Canada, scheduled for demolition. The building, shown in Fig. 1, was built in the late 19th century as a wood structure, with masonry walls of the type described above. The plan dimensions of the building were 14 m × 9 m. The timber structure consisted of stacked 75 mm × 250 mm (3 in. × 10 in.) rough-cut timber planks laterally supported by vertical posts at 4 m (12 ft) spacing. In addition

FIG. 1. Three-Story Older Residential Building in Montreal, Canada from Which Wall Specimens Were Retrieved

[1]Grad. Res. Asst., Ottawa Carleton Earthquake Engrg. Res. Ctr., Dept. of Civ. Engrg., Univ. of Ottawa, 161 Louis Pasteur, Ottawa, ON, Canada, K1N 6N5. E-mail: jpaqu044@uottawa.ca

[2]Prof. and Deputy Dir. of Multidisciplinary Ctr. for Earthquake Engrg. Res., Dept. of Civ. Struct. and Envir. Engrg., 130 Ketter Hall, State Univ. of New York at Buffalo, Buffalo, NY 14260. E-mail: bruneau@acsu.buffalo.edu

[3]Prof., Div. of Struct. Engrg., Univ. of California at San Diego, 9500 Gilman Dr., Mail Code 0085, La Jolla, CA 92093. E-mail: afiliatrault@ucsd.edu

Note. Associate Editor: Brad Cross. Discussion open until October 1, 2001. To extend the closing date one month, a written request must be filed with the ASCE Manager of Journals. The manuscript for this paper was submitted for review and possible publication on June 14, 2000; revised November 30, 2000. This paper is part of the ***Journal of Structural Engineering***, Vol. 127, No. 5, May, 2001. ©ASCE, ISSN 0733-9445/01/0005-0561–0569/$8.00 + $.50 per page. Paper No. 22428.

FIG. 2. Retrieval of Test Specimens from Existing Building

to the four single-wythe brick masonry exterior facades of the building, two more walls of the same construction became interior walls when an addition was built a few years after the original construction. The specimens were extracted from a single interior wall for which access to both sides was facilitated, and to minimize variability of construction. Note that for these interior walls, a thin layer of plaster covered the brick surface and had to be removed prior to the shake table tests.

Careful retrieval of the specimens was critical to maintain the integrity of the masonry wall and wood-backing assemblies during extraction and transportation. First, horizontal saw cuts, 1.2 m long and spaced at 2 m vertically, were made through each wall. Steel plates with predrilled holes were inserted in each cut. Four steel threaded rods were tightly bolted between the plates, on each side of the wall. A plywood sheet was placed on each surface of the wall, and wedged by timber members against the threaded rods. The bottom portion of the wall underneath the bottom cut was demolished to the floor level. A rolling cart was introduced in the opening and secured to the bottom steel plate. Finally, the vertical sections of the specimen were saw cut. The crated specimen was rolled out of the wall and retrieved from the building by a boomed truck, as shown in Fig. 2.

Basic tests were conducted to determine the material properties of the masonry specimens. First, before retrieval of the specimen, an in-place shear test was performed directly on the interior wall in accordance with the special procedure of Appendix A of the *Uniform code for building conservation* (*UCBC*) (International 1997). A mortar shear strength of 0.401 MPa was obtained, which exceeds the minimum value of 0.2 MPa, for which repointing would have been required. Also, masonry specimens were cut out of the interior walls and brought to the laboratory for flexural tension and compression tests. Due to the fragility and particular geometry of the specimens available, special tests were devised to determine these basic properties. A three-point bending test was performed on two bricks bonded by an uncracked mortar joint, followed by a compression test on the same. The obtained compressive (f'_m) and tensile (f_t) strengths of the masonry were 2.50 MPa and 0.0162 MPa, respectively.

RETROFIT TECHNIQUES

One of the three wall specimens was tested in its existing condition, as shown in Fig. 3(a); the other two were retrofitted prior to testing. The first retrofit strategy consisted of adding through-thickness anchors connecting the masonry to the wood backing. The intent was to determine if it is possible to rely on the stiffness of the wood backing to reduce the height-to-thickness ratio of the wall by intermediate anchorages. Here, two bolts were used at the midheight of the specimen. Cintec bolts with socks injected with grout under pressure (*Cintec* 1996) were used to ensure a bearing surface over the expanded sock surface in the gap between the masonry and the timber planks.

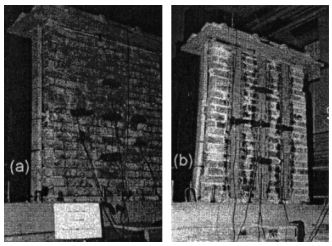

FIG. 3. Specimens: (a) As-Built Specimen; (b) Specimen Retrofitted with Tyfo Fiberglass Strips

In the second retrofit strategy, fiberglass strips (Tyfo 1997) were glued to the masonry side of the wall, to increase its out-of-plane stiffness and strength. As shown in Fig. 3(b), three vertical strips 102 mm wide were epoxied to the masonry surface of the wall specimen. Although retrofitting both sides of the walls with strips is typically recommended based on available testing results (Reinhorn and Madan 1995), this is not possible for the type of construction considered herein. Nevertheless, the expectation for the single-side retrofit of this specimen was that the fiberglass strips would prevent dynamic out-of-plane instability of the masonry in the outward direction, and that the wood backing would preclude the same in the inward direction, in spite of the small gap present between the two walls. Such a retrofit assumption can only be experimentally verified by shake table testing.

EXPERIMENTAL PROCEDURE

Test Setup and Instrumentation

The shake table tests were performed on the uniaxial earthquake simulation facility at Ecole Polytechnique in Montreal (Filiatrault et al. 1996). As shown in Fig. 4, a rigid steel A-frame was used to tie the top of the wall, whereas the bottom was cast into a concrete base bolted to the shake table. This was to ensure that both the top and the bottom of the wall would be subjected to the same seismic excitation, as commonly assumed for the upper stories when performing seismic evaluation of unreinforced masonry buildings incorporating wood floor diaphragms (ABK 1984; Bruneau 1994; International 1997). The top of the wall was secured to the A-frame by two steel angles welded to the wall's top steel plate in-

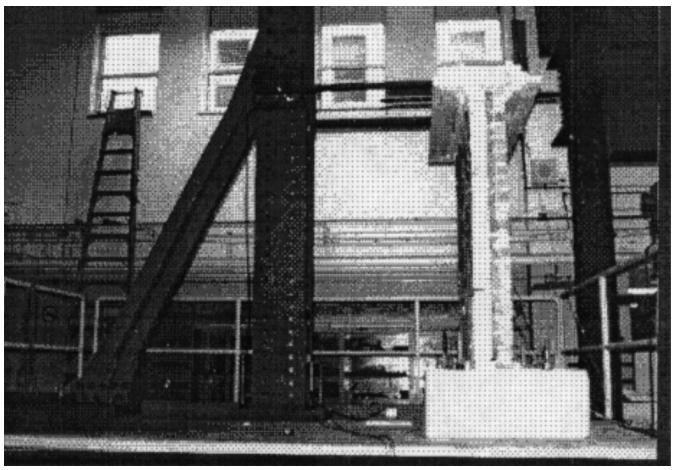

FIG. 4. Test Setup on Shake Table

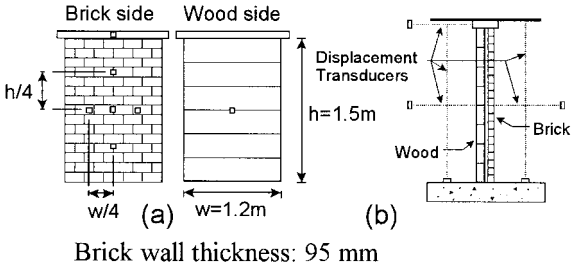

FIG. 5. Location of: (a) Accelerometers; (b) Displacement Transducers on Specimens

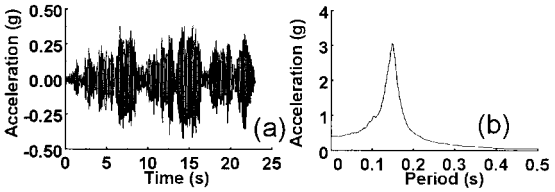

FIG. 6. Floor-Level Seismic Input Motion for Shake Table Tests: (a) Acceleration Time History: (b) Absolute Acceleration Response Spectrum at 5% Damping

stalled prior to transportation. This plate was bolted to a wooden belt surrounding the top edge of the wall. This belt was installed prior to removing the steel threaded rods and plywood panels used for crating. These plywood panels were saw cut at the concrete base level and just below the wooden belt, revealing the specimen and permitting removal of the thin layer of plaster covering the brick surface. The final net dimensions of the wall specimens were approximately 1.2 m × 1.5 m. The measured thickness of the brick wall was 95 mm. The initial gap between the wood backing and the brick wall varied from 15 to 20 mm for both the as-built specimen and the Cintec specimen. The Tyfo specimen was initially in poor condition compared to the other two specimens. The brick wall had several cracks through the mortar joints and the bricks themselves. Contrary to the previous specimens, two of the timber planks in the wood backing were not continuous (i.e., a joint was present). Also, part of the wood backing was slightly charred (hinting of prior fire damage) and the initial gap between the wood and brick wall was larger, varying from 25 to 35 mm. These conditions were not repaired prior to application of the Tyfo strips and were not considered to be significant factors in the dynamic performance of the test specimens. Since the masonry walls typically resisted only their self weight in the existing building and because top story walls are typically more vulnerable during earthquakes (Bruneau 1995), no supplementary gravity load was considered for the shake table tests.

Horizontal acceleration time histories at different locations on the specimen were measured using seven accelerometers. All except one were located on the brick wall, as shown in Fig. 5(a). Additionally, five displacement transducers were used to measure horizontal and vertical movements, as shown in Fig. 5(b). All data were recorded automatically by a data acquisition system at a sampling rate of 200 readings per second per channel.

Testing Sequence

The three wall specimens were subjected to the same seismic input motion of progressively increasing intensity, expressed in terms of peak horizontal acceleration (PHA), until structural failure was observed. Between each seismic excitation, low level impact tests were performed by hammering the wall with a bare fist to capture the evolution of the wall's out-of-plane dynamic characteristics (natural frequencies, mode shapes, and damping ratios). The natural frequencies were determined from power spectral density plots of the absolute acceleration records on the walls. The structural mode shapes were obtained from the amplitudes of the spectral peaks, and by the phase and coherence between the measured acceleration time histories. The first modal damping ratio of the wall specimen was then established by the logarithmic decrement method (Clough and Penzien 1993).

To determine an appropriate floor-level seismic input motion for the shake table tests, linear dynamic time-history analyses were performed on a typical one-story unreinforced masonry building incorporating a wooden floor diaphragm. These analyses were performed for the following four different ground motions: (1) the S00E component of the 1940 El Centro earthquake; (2) the N24E component of the ground motion recorded at Chicoutimi North during the 1988 Saguenay earthquake in Quebec; (3) a synthetic ground motion compatible with the short periods of the recently proposed uniform hazard spectrum for Montreal (Atkinson and Beresnev 1998); and (4) a synthetic ground motion compatible with the long periods of the same uniform hazard spectrum for Montreal (Atkinson and Beresnev 1998).

Based on the results obtained, the acceleration time history obtained at the floor level of the analyzed building under the synthetic long period accelerogram for Montreal was selected for the shake table tests. The acceleration time history and the associated absolute acceleration response spectrum, at 5% damping, for this floor motion are presented in Fig. 6. It can be seen that most of the energy of the signal is concentrated in the 0.15 s period range, corresponding to the natural period of the building analyzed. Note also that the full-scale amplitude of the selected floor motion has a PHA value of 0.40*g*, corresponding to a peak ground acceleration (PGA) of 0.13*g*.

THEORETICAL STRENGTH OF WALL SPECIMENS

Prior to testing, the expected out-of-plane strength of the wall specimens was assessed using three different approaches. First, it is possible to deduct the strength of a masonry wall subjected to out-of-plane excitation from the limits of the *h*/*t* ratio specified by code documents such as the Canadian ''Guidelines for seismic evaluation of existing buildings'' (CGSEEB) (National 1992) and the *UCBC* (International 1997). Here, the *h*/*t* ratio of the masonry wall in these specimens is 15.2. Specified limits in the CGSEEB indicate that the wall specimens can survive earthquakes in regions of effective zonal velocity ratio z' of 5 or less, which translates into a maximum peak ground velocity (PGV) of 0.32 m/s and a PGA of 0.32*g*. Considering implied amplification velocity values of 1.75, this corresponds to floor velocities of 0.56 m/s.

Second, a probabilistic assessment is possible by considering the data supporting the ABK methodology (ABK 1984; Bruneau 1994), from which other procedures such as the *UCBC* and CGSEEB are directly derived. For the given *h*/*t* ratio of 15.2, and absence of overburden on the tested wall (i.e., no axial load applied), the floor velocity applied to the wall can be related to a specified probability of survival. Here, for a 98% probability of survival, the peak floor velocity (assuming identical velocities applied at the top and bottom of the wall) is 0.538 m/s. For a 50% probability of survival, this increases to 0.574 m/s. The corresponding peak ground acceleration for 98% and 50% survival would be 0.307*g* and 0.328*g*, respectively.

Finally, using a method proposed by Priestley (1985; Priestley and Paulay 1992) to calculate dynamic out-of-plane wall stability, the accelerations (uniformly distributed along the height of the wall) to initiate cracking and to trigger static instability were calculated to be 0.044*g* and 0.108*g*, respectively. This result, obtained considering an elastic nonlinear

model, is then converted using an equal energy approach into a corresponding value for an equivalent linear elastic model. This equivalent elastic lateral wall response acceleration to induce failure was thus calculated to be 2.58*g*.

Strength estimates for the wall retrofitted using Cintec anchors depend on whether the anchors provided at midheight of the wall are effective in reducing the *h*/*t* ratio by a factor of 2. Assuming full effectiveness for the sake of comparison, then, according to the CGSEEB and *UCBC*, the wall could survive earthquakes in regions of effective zonal velocity ratio z' of 6, corresponding to PGV and PGA in excess of 0.4 m/s and 0.4*g*, respectively. According to the Agbabian Barnes Kariotis methodology, for 98% and 50% survival, the peak velocity at each end of the wall would be 0.683 m/s and 0.790 m/s, respectively. The corresponding peak ground acceleration for 98% and 50% survival would be 0.390*g* and 0.451*g*, respectively. Based on Priestley's method, the equivalent elastic lateral wall response acceleration at failure would be 15.4*g*.

For the wall retrofitted with Tyfo fiberglass strips, ultimate capacity was computed using a reinforced-concrete stress block analogy, but where the steel reinforcement is replaced by the fiberglass. The corresponding lateral wall acceleration at failure was found to be 6.02*g*.

EXPERIMENTAL RESULTS

Descriptions and visual observations made during the testing of each specimen are presented in this section. Each wall specimen was subjected to the same seismic input motion of progressively increasing intensity starting at 0.05*g*, increasing by increments of 0.05*g* up to 0.20*g*, then by increments of 0.10*g* up to 0.40*g*, and by 0.20*g* increments up to 1.0*g*, and 0.25*g* afterward until failure. A video camera was used to record global specimen behavior during the tests. After each test run, the condition of each specimen and the extent of cracking were noted, and photographs were taken.

As-Built Specimen

Up to a PHA of 0.15*g*, the response of the as-built specimen was characterized by very small vibrations, making the deflected shape barely perceptible. Minor cracks extended from existing cracks on the left side of the brick wall. At 0.15*g*, the dynamic response was more visible, as well as the deflected shape. Two cracks appeared in the central portion of the wall. From 0.2*g* to 0.6*g*, the brick wall deflections gradually increased, which formed new cracks and extended existing ones,

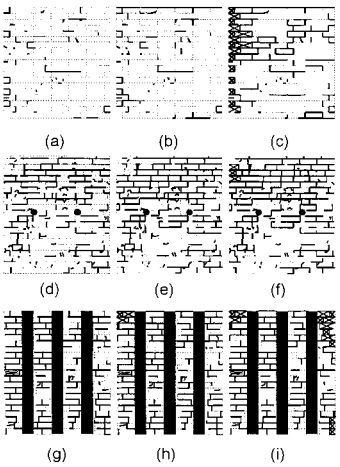

FIG. 7. Crack Pattern for As-Built Specimen at PHA of: (a) 0.4*g*; (b) 1.0*g*; (c) 1.5*g*. Cintec Specimen at PHA of: (d) 0.4*g*; (e) 1.0*g*; (f) 1.5*g*. Tyfo Specimen at PHA of: (g) 0.4*g*; (h) 1.0*g*; (i) 1.5*g* [Fallen Bricks Are Covered by an X; Solid Circles in (d), (e), and (f) Indicate Anchors]

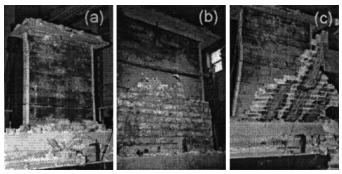

FIG. 8. Failure Mode of: (1) As-Built Specimen; (b) Cintec Specimen; (c) Tyfo Specimen

as shown in Fig. 7(a). A parabolic deflected shape could be clearly seen during the response. At 0.8*g*, the response became more severe and dust emanated from the plaster inside the wooden belt. A full-width crack formed at the top just below the wooden belt, causing the wall to behave slightly more like a mix of a cantilever and simply supported beam. At 1.0*g*, a more severe response caused the plaster cover that was hidden inside the wooden belt to crumble, creating further dust. Due to the full-width crack at the top, as shown in Fig. 7(b), the wall was now sliding under the top row of brick. After a PHA of 1.25*g*, several cracks around numerous bricks were noticeable, mostly on the upper left portion of the wall, but no bricks had fallen. However, at a PHA of 1.5*g*, most of these bricks fell, as shown in Fig. 7(c), leaving the specimen in poor condition. At 1.75*g*, the as-built specimen completely failed, as shown in Fig. 8(a). Starting from the upper rows, all bricks fell down successively. The wood backing was still standing, and after close inspection, wood mortises were discovered between the 75 mm × 250 mm (3 in. × 10 in.) planks on the right side only.

Cintec Specimen

Up to 0.6*g*, the response of the Cintec specimen was identical to that of the as-built specimen, with the exception that being attached with anchors, the wood backing could clearly be seen moving along with the brick wall. At 0.8*g*, the portion of the wall above the anchors was noticed to respond more, as evidenced by the more extensive cracking developing above midheight compared to the lower portion, as shown in Figs. 7(d) and 7(e). At 1.0*g*, dust emanated from the upper portion of the brick wall. After a PHA of 1.25*g*, cracks were found almost around each brick, especially in the upper part of the wall. As shown in Fig. 7(f), at 1.5*g*, three bricks on the upper left side fell down. The mortar joints in the first four rows of brick at the top were thoroughly cracked and pieces had fallen down, leaving these bricks in precarious stability. The nails connecting the brick wall to the wood backing above the anchors were sliding freely in the mortar joints. At a PHA of 1.75*g*, the upper portion of the Cintec wall fell down, leaving the part below the anchors in relatively good condition, as shown in Fig. 8(b). No wood mortises were discovered in the wood backing.

Tyfo Specimen

From a PHA of 0.05*g* to 0.20*g*, the wall responded almost rigidly, with almost no visible deflection. No new cracks appeared during these test runs. After a PHA of 0.30*g*, pieces of mortar fell down, leaving some bricks in the upper corner considerably unstable. Also, a small gap was noticed in the wooden belt between the plywood and the encased brick wall. From a PHA of 0.40*g* to 0.80*g*, the gap inside the wooden belt grew, causing the brick wall to behave more like a cantilever partially restrained at the top. During each test run, pieces of mortar were falling in the cavity between the brick and wood wall, and several bricks on each side at the top became very unstable. After 0.80*g*, the remaining piece of crated plywood inside the wooden belt was displaced upon repeated impact, as shown in Fig. 9. After 1.0*g*, bricks fell from the upper left side and from inside of the wooden belt, as shown in Figs.

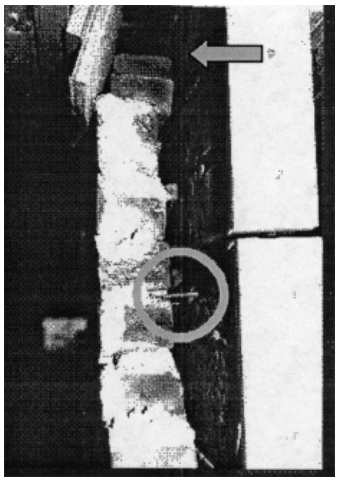

FIG. 9. Lack of Tight Fit inside the Wooden Belt at the Top of the Wall due to Repeated Shaking (Arrow), and Connecting Nails Embedded in Mortar Joints (Circle)

7(g) and 7(h). At 1.25*g*, other bricks fell from the upper and bottom right corners, as shown in Fig. 7(i). The accumulation of mortar debris in the cavity between the two walls was rising above midheight. After a PHA of 1.5*g*, more bricks fell from the right side and from inside the wooden belt. At this point, there was a considerable gap inside the wooden belt, allowing the wall to behave first as a cantilever, until it hit the side of the belt, and then as a simply supported wall following that impact. The upper left portion only of the wall fell at a PHA of 1.75*g*, tearing a Tyfo strip above midheight in the process. The remaining portion of the wall stayed in place due to the other Tyfo strips being glued to the remaining piece of crated plywood inside the wooden belt. At 2.0*g*, the Tyfo strips debonded from the plywood, causing the remaining portion of the brick wall to fall like a rigid body held together by fiberglass strips, as shown in Fig. 8(c). Although difficult to quantify, it is expected that some improvement in behavior would have been observed if, for each specimen, the test at the highest PGA had been carried out without prior shaking at increasing amplitudes.

VARIATION OF DYNAMIC PROPERTIES

Fundamental Frequencies

As shown in Fig. 10(a), the fundamental frequency of the as-built specimen gradually decreased, from 6.25 Hz initially to 5.66 Hz at a PHA of 0.6*g*. At 0.8*g*, the frequency dropped to 4.59 Hz, due to development of a full-width crack at the top, to reach 4.00 Hz at 1.25*g*. It then increased to 4.29 Hz at

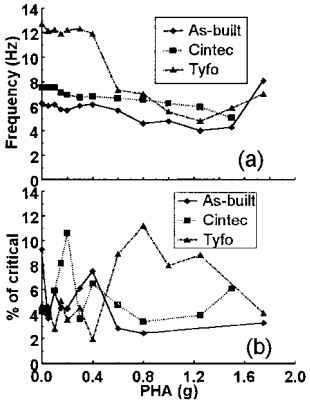

FIG. 10. Variation of Dynamic Properties: (a) Fundamental Frequencies; (b) Damping Ratios

1.5*g* as several bricks fell, thereby reducing the effective mass of the wall. After failure of the brick wall, the frequency of the wood backing alone was found to be 8.1 Hz.

The initial natural frequency of the Cintec specimen was 7.52 Hz, and did not change during the first few test runs. At a PHA of 0.15*g*, it gradually decreased to 5.1 Hz at failure of the wall.

The initial frequency of the Tyfo specimen was 12.7 Hz. Up to 0.4*g*, the natural frequency remained almost constant. At 0.6*g*, it dropped to 7.32 Hz due to the gap created in the connection at the top, and then gradually decreased to 4.79 Hz. It increased to 5.85 Hz and 7.03 Hz at a PHA of 1.5*g* and 1.75*g*, respectively, as the specimen began to lose bricks and due to the ample accumulation of debris in the cavity between the two walls.

Damping Ratios

The damping ratio, measured as described in an earlier section, varied considerably for each wall and between each test run, ranging from 2% to 11%, as shown in Fig. 10(b). The initial damping of the as-built specimen ratio was 9.3%; it dropped to about 4.5% for the first few test runs, increased to 7.5% at a PHA of 0.4*g*, then dropped to about 3% for the remainder of the tests. The damping ratio of the wood backing alone was found to be 3.28%. The initial damping ratio of the Cintec specimen was approximately 4%; it increased to 10% at a PHA of 0.2*g*, dropped to 3.6% at 0.3*g*, then progressively decreased from 6.5% at 0.4*g* to 3.5% at a PHA of 0.8*g*, and finally increased to 6.1% at 1.5*g*. The initial damping ratio of the Tyfo specimen was 4.75%; it dropped to 2.75% and 2% at a PHA of 0.1*g* and 0.4*g*, respectively, with some higher values recorded in between, increased to 11.2% at a PHA of 0.8*g*, and gradually decreased to 4% at 1.75*g*. The considerable variation of damping ratios is attributed to the small numbers of low amplitude cycles used to calculate these values. As such, from Fig. 10(b), one could argue that damping, on average, has not varied meaningfully during these tests (i.e., no clear trend could be established), and that average values of 5.2%, 5.6%, and 5.7% for the as-built, Cintec, and Tyfo specimens, respectively, could have been used.

Mode Shapes—Vertical Profiles

Using the data recorded by the accelerometers located on the wall, the fundamental mode shapes were generated at various steps throughout the testing sequence. The first tests yielded a parabolic shape for the as-built specimen, as shown in Fig. 11(a). The curvature was not perfectly symmetric about midheight due to a less rigid connection at the top compared to the bottom, where it was cast into concrete. Based on trial and error, the mode shape and period of a fixed-pinned model more closely match the experimental results than do any other simple assumptions (e.g., pinned-pinned), even though some discrepancy is noted in the lower part of the mode shapes. The

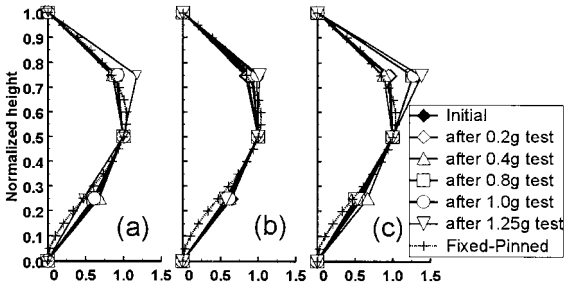

FIG. 11. Mode Shapes of: (a) As-Built Specimen; (b) Cintec Specimen; (c) Tyfo Specimen

mode shape was constant up to a PHA of 1.0*g*. At a PHA of 1.25*g* and higher, the response of the upper part of the wall started to exceed that of midheight, eventually causing failure of the wall.

The mode shape of the Cintec specimen is similar to that of the as-built specimen. As shown in Fig. 11(b), at a PHA of 1.0*g* and 1.25*g*, the displacement at the 3/4 height nearly equals that at midheight and is comparable to that of the as-built specimen, suggesting that the anchors at midheight did not noticeably help to prevent excessive displacement of the upper portion of the wall. Nonetheless, the flexible connection at the top caused the wall to fail prematurely.

For the first test runs of the Tyfo specimen, the mode shape was very similar to that of the previous specimen as shown in Fig. 11(c). However, the mode shape changed radically when a gap developed in the wooden belt. As described earlier, the wall then started to behave like a cantilever, banging at the top inside the wooden belt. The deteriorating conditions at the top subsequently led to the wall failure.

Mode Shapes—In-Plan Deformations

Using the accelerometers located across the width of the specimen at midheight, the in-plan mode shapes were generated. As shown in Fig. 12, some torsion was experienced by the specimens during each test. It is clearly evident on the as-built specimen, for which a larger displacement is noticed on the left side in most test runs. This is consistent with the observation that cracks developed primarily on this side of the wall during testing. When the specimen was removed from the shake table, vertical wood mortises were discovered between planks only on the right side of the wall. The Cintec retrofit specimen, which had no wood mortises in the wood backing, showed a small amount of torsion compared to the as-built specimen. A similar observation can be made for the Tyfo retrofit specimen, which exhibited very little torsion in spite of the substantially poor initial conditions of the brick wall.

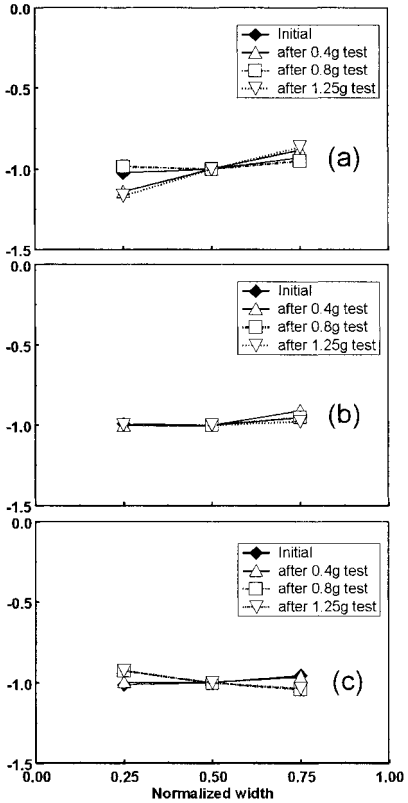

FIG. 12. Mode Shapes In-Plan of: (a) As-Built Specimen; (b) Cintec Specimen; (c) Tyfo Specimen

ANALYSIS OF RESULTS

Wall Response

The existing unreinforced masonry wall was able to resist significant peak horizontal accelerations without substantial damage. As shown in Figs. 13(a) and 13(b), large accelerations developed at the midheight of the wall before they collapsed out of plane. Note that the wall's dynamic response significantly amplified the input floor accelerations, as shown in Figs. 13(c) and 13(d). As the level of excitation increased from 0.05*g* to 1.25*g*, the amplification at midheight of the as-built specimen decreased from 3.16 to 0.86, respectively. Based on the experimental values for the period and damping ratio, theoretical corresponding wall dynamic amplifications for each specimen were calculated and compared against the values obtained experimentally, as shown in Fig. 14. It can be seen in

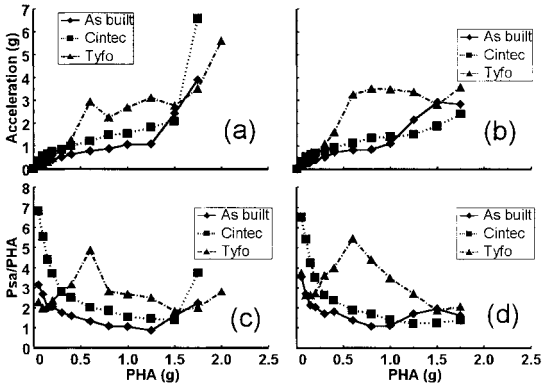

FIG. 13. Peak Acceleration at Center of Wall: (a) Brick Side; (b) Wood Side. Dynamic Amplification Factor at Center of Wall: (c) Brick Side; (d) Wood Side

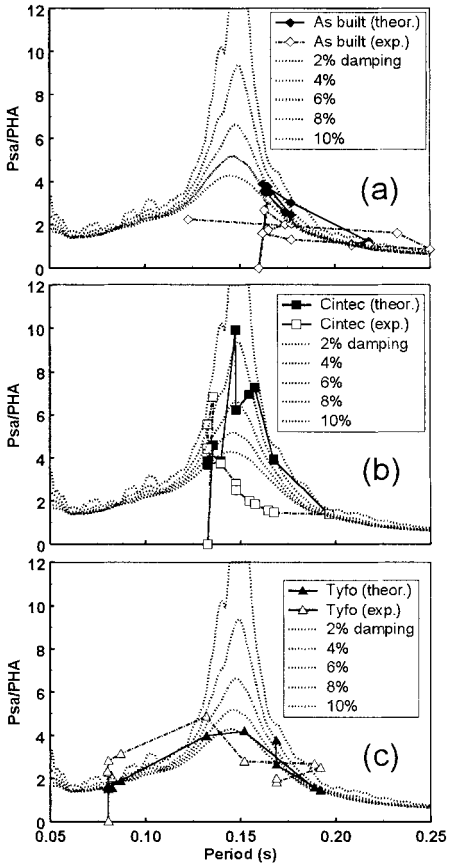

FIG. 14. Response Spectrum of: (a) As-Built Specimen; (b) Cintec Specimen; (c) Tyfo Specimen

Fig. 14(a) that the initial period of the as-built wall was located right after the spectral peak; therefore, as the period elongated, the dynamic amplification from the wall decreased. The Cintec specimen, being more rigid (i.e., having a shorter period), had an amplification factor of 6.82 initially; it decreased accordingly as the period lengthened, even though the initial period of the Cintec wall was located just before the peak response, as shown in Fig. 14(b). Interestingly, the behavior of the Tyfo retrofit was different. The specimen had a considerably shorter period than the other two specimens. As the period lengthened, the amplification factor increased from 2.28 initially to 4.87

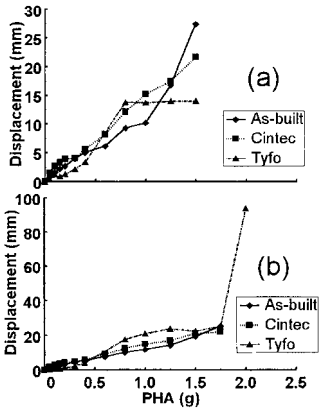

FIG. 15. Peak Displacement at Center of Wall: (a) Brick Side; (b) Wood Side

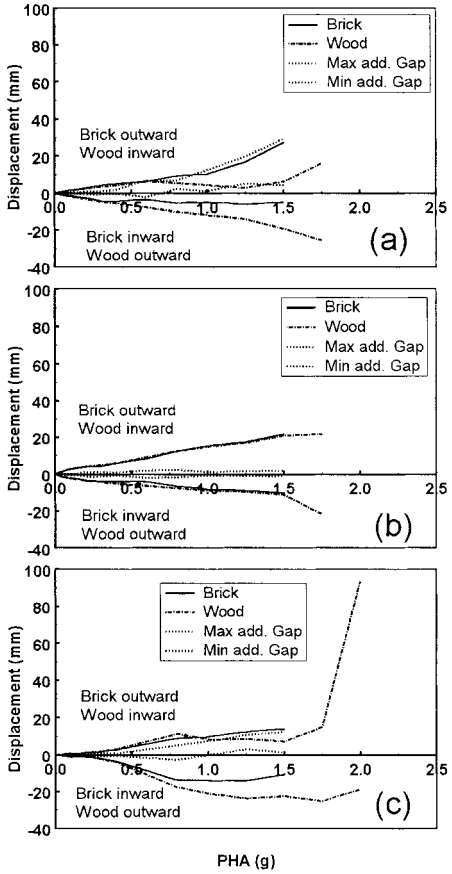

FIG. 16. Maximum Inward and Outward Displacement, and Progression of Gap between Wood and Brick Wall at Midheight of Wall for: (a) As-Built Specimen; (b) Cintec Specimen; (c) Tyfo Specimen. Maximum Additional Gap Indicates the Largest Increase in the Distance between the Masonry and Wood Wall, at Midheight, at Any Time and in Any Direction during the Response Time History. Minimum Additional Gap Is the Corresponding Smallest Increase (If Positive), or Largest Decrease (If Negative)

at a PHA of 0.6*g*, then decreased to 1.84 at a PHA of 1.5*g*, as shown in Fig. 13(c). By looking at the response spectrum as shown in Fig. 14(c), one can see that the actual peak of the response spectrum as observed experimentally was found to be at a period of approximately 0.133 s instead of 0.15 s, which is concordant with the behavior observed for the Cintec and Tyfo specimens.

As shown in Figs. 15(a) and 15(b), the lateral maximum displacement at midheight increased as the level of input seismic motion increased. This increase is almost linear in the case of the as-built and Cintec specimens, except for a PHA greater than 1.0*g* for the as-built specimen, where maximum displacement increases more significantly. The maximum displacement of the Tyfo specimen at midheight appears to be nonproportional and limited to a certain value (approximately 14 mm) after a PHA of 0.8*g*. This is explained by Fig. 16, where the maximum inward and outward displacements of both the brick wall and the wood backing during testing are presented. It can be seen in Fig. 16(c) that, at a PHA of 0.8*g* and 1.0*g*, the inward displacement, which was greater than the outward displacement, was limited when the brick wall was moving toward the wood backing.

Wood-Masonry Interaction

As shown in Fig. 16(a), the wood backing and brick wall of the as-built specimen were moving in-phase during the first test runs (as indicated by the brick and wood displacement curves closely following each other), and were moving more independently of each other as the level of excitation increased. As mentioned earlier, the wood and brick walls were connected together only by nails protruding from the wood backing and embedded in the masonry walls' mortar joints. As the level of earthquake intensity increased, these nails started to slide freely in the mortar. The gap between the wood and brick walls, originally 15–20 mm, expanded by an additional 29.7 mm.

As shown in Fig. 16(b), introducing anchors at midheight forced the two walls to move together and kept the gap between them from increasing noticeably during the test, with the additional gap generated being only 2.0 mm. Another way to confirm this behavior is by looking at the phase angle. By comparing the frequency content of the accelerometers located at midheight of the brick wall and wood backing, it is possible to determine the phase relation between the two walls. A phase angle of 0° means that both walls are moving in-phase, whereas an angle of 180° indicates that they are completely out-of-phase. Thus, as observed in Fig. 17, the phase angle is almost zero throughout the test for the Cintec specimen compared to the as-built specimen, which increased almost exponentially after a PHA of 1.0*g*. Interestingly, the fiberglass retrofit apparently also helped to keep the two walls together, even though no improvements were made to the nail connection. The additional gap observed in that case was about 12.3

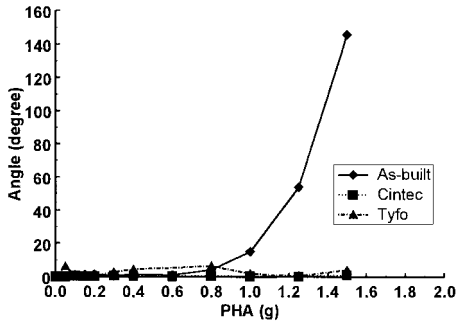

FIG. 17. Variation of Phase Angle

mm, adding to an initial gap of 25–35 mm, as shown in Fig. 16(c).

COMPARISON WITH ANALYTICAL PREDICTIONS

The base acceleration that caused the collapse of the as-built wall was 1.75*g*, corresponding to a wall base and top velocity of 0.404 m/s and a PGA of 0.583*g*, given a floor amplification of 3 obtained from the diaphragm linear dynamic analyses. This result is lower than the 0.538 m/s and 0.574 m/s values for 98% and 50% probability of survival predicted by the ABK methodology. However, it exceeds the 0.32*g* maximum PGA capacity calculated by the CGSEEB in an earlier section. The peak acceleration value recorded at midheight was 3.92*g* at a PHA of 1.75*g*, a value greater than 2.58*g*, the lateral response acceleration calculated by Priestley's method.

Specified limits in the CGSEEB indicated that the Cintec specimen could survive to a maximum PGA of 0.4*g* or higher if the anchors at midheight were effective in reducing the *h*/*t* ratio by two. As exhibited by the mode shape in an earlier section, the anchors did not effectively contribute to reducing the *h*/*t* ratio, but helped to increase the structural integrity of the specimen. However, like the as-built specimen, the Cintec wall collapsed at a base acceleration of 1.75*g*, corresponding to a wall base and top velocity of 0.404 m/s, which is lower than the values predicted by the ABK methodology, as stated above. The peak lateral acceleration recorded at midheight was 6.58*g* at a PHA of 1.75*g*, a value greater than 2.58*g* but lower than 15.4*g*, as calculated by Priestley's method for a wall with an *h*/*t* ratio reduced by two.

The peak lateral acceleration recorded at midheight for the Tyfo specimen at collapse was 5.59*g* at a PHA of 2.0*g*. This result is lower than the 6.02*g* value predicted in an earlier section, based on a reinforced-concrete stress block analogy.

It is important to remember when interpreting the experimental results that they are from wall specimens whose heights (1.5 m) are not representative of the actual floor-to-floor distance in buildings. A height of approximately 2.5–3.0 m is more likely for a masonry wall panel spanning vertically between floor diaphragms. In such cases, the *h*/*t* ratio may range from 25 to 30, which exceeds the limit of 20 specified in the CGSEEB and *UCBC*. Therefore, such walls would survive earthquakes in regions of effective zonal velocity ratio z' of 1 or less, which translates into a maximum PGV of 0.08 m/s and PGA of 0.08*g*. According to the ABK methodology, for 98% and 50% survival, the peak velocity at each end of the wall would be 0.377 m/s and 0.413 m/s, respectively. Based on Priestley's method, the equivalent lateral response wall acceleration at failure would be 0.357*g*. All these values are significantly less than those calculated for the test specimens.

Various analytical procedures have been tried in attempts to model the experimental behavior observed. A model by Blaikie and Davey (2000) was first considered. They have studied the seismic behavior of face loaded unreinforced masonry walls, modeled the walls as uncracked except at the diaphragm and midheight levels, and assessed their stability under lateral load using simple statics in the deformed configuration. The lateral load deformation calculated using this model for the as-built wall is plotted in Fig. 18. Note that while this model takes into account the self-weight and overburden load from a parapet or any upper story as contributing to the stability, the wall model is not restrained against vertical movements due to rigid body motions on open cracks. A model developed by Priestley includes the effects of stiff boundary conditions in which compression struts are formed as the wall cracks under lateral inertial accelerations. The corresponding membrane compression deformation relationship for the as-built wall is plotted in Fig. 18 and could be viewed as an upper-bound limit. It appears that experimental results partly progressed toward the upper limit, as shown in Fig. 18, and largely exceeded the values predicted by the Blaikie and Davey model. However, it was observed during testing that while the specimens were restrained at the top, the lack of tight fit provided by the wooden belt increased as the level of seismic excitation increased. Therefore, the resistance provided by compression membrane action diminished until the upper brick portion of the wall sustained large displacements that triggered dynamic instability, causing the collapse of the wall.

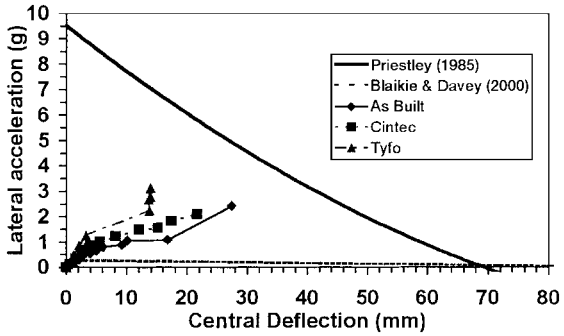

FIG. 18. Comparison of Lateral Acceleration–Displacement Response at Midheight with Various Analytical Models

CONCLUSION

Out-of-plane shake table tests have been conducted on three existing unreinforced masonry walls with wood backing assemblies. These tests have demonstrated that such walls could resist significant out-of-plane inertial accelerations without failure. Performance can be increased by different retrofit methods such as providing anchors at midheight to force the wood and masonry wall to move as a unit, and adding fiberglass strips epoxied to the masonry wall to increase its out-of-plane stiffness and strength. The latter method proved to be more effective. However, in order to achieve such out-of-plane performances for wall panels, it is assumed that the walls are properly anchored at the floor/roof levels. Otherwise, as shown in the tests, lack of appropriate boundary conditions could considerably reduce expected performance. Various analytical methods have been used to explain the observed behavior, but the lack of tight fit at the top of the wall in the test setup and interaction with the wood backing resulted in an intricate ultimate failure mode that could not be replicated analytically.

ACKNOWLEDGMENTS

The writers gratefully acknowledge the following organizations for their technical and financial assistance in this project: Cintec Canada, Composite Retrofit International (Tyfo S Fibrwrap System), the National Science and Engineering Research Council of Canada, and the Fonds de Formation des Chercheurs et D'aide à la Recherche of Quebec.

REFERENCES

ABK, a Joint Venture. (1984). ''Methodology for mitigation of seismic hazards in existing unreinforced masonry buildings: The methodology.'' *Rep. ABK-TR-08*, Agbabian & Associates, S.B. Barnes & Associates, and Kariotis & Associates, El Segundo, Calif.

Atkinson, G. M., and Beresnev, I. A. (1998). ''Compatible ground-motion time histories for new national seismic hazard maps.'' *Can J. Civ. Engrg.*, Ottawa, Canada, 25(2), 305–318.

Blaikie, E. L., and Davey, R. A. (2000). ''Seismic behaviour of face loaded unreinforced masonry walls.'' *12th World Conf. on Earthquake Engrg.*, New Zealand Society for Earthquake Engineering, Silverstream, Upper Hutt, New Zealand.

Bruneau, M. (1994). ''Seismic evaluation of unreinforced masonry build-

ings—A state-of-the-art report.'' *Can J. Civ. Engrg*., Ottawa, Canada, 21(3), 512–539.
Bruneau, M. (1995). ''Performance of masonry structures during the 1994 Northridge (Los Angeles) earthquake.'' *Can. J. Civ. Engrg*., Ottawa, Canada, 22(2), 378–402.
Cintec international news. (1996). Cintec Canada, Nepean, Ont., Canada.
Clough, R. W., and Penzien, J. (1993). *Dynamics of structures*, 2nd Ed., McGraw-Hill, New York.
Filiatrault, A., Tremblay, R., Thoen, B. K., and Rood, J. (1996). ''A second-generation earthquake simulation system in Canada: Description and performance evaluation.'' *11th World Conf. on Earthquake Engrg., Paper No. 1204*.
International Conference of Building Officials (ICBO). (1997). *Uniform code for building conservation*, Whittier, Calif.
National Research Council (NRC). (1992). ''Guidelines for seismic evaluation of existing buildings.'' Institute for Research in Construction, Ottawa, Canada.
Priestley, M. J. N. (1985). ''Seismic behaviour of unreinforced masonry walls.'' *Bull. New Zealand Nat. Soc. for Earthquake Engrg*., Waikanae, New Zealand, 18(2), 191–205 and 19(1), 65–75.
Priestley, M. J. N., and Paulay T. (1992). *Seismic design of reinforced concrete and masonry buildings*, Wiley, New York.
Reinhorn, A. M., and Madan, A. (1995). ''Evaluation of Tyfo-W Fiber Wrap system for out-of-plane strengthening of masonry walls.'' *Rep. No. 95-AM-0001*, Department of Civil Engineering, State University of New York, Buffalo, N.Y.
Tyfo Systems. (1997). ''For unreinforced masonry (URM) and reinforced concrete/masonry wall strengthening.'' Fyfe Company L.L.C., San Diego.